



OPEN

Quantum modeling simulates nutrient effect of bioplastic polyhydroxyalkanoate (PHA) production in *Pseudomonas putida*

Lawrence Yuk Lung Ho¹, Li Pan², Fei Meng³, Kin Tung Michael Ho⁴, Feiyang Liu³, Ming-Tsung Wu⁴, Hei I. Lei⁴, Govind Bhachu⁴, Xin Wang³, Oscar Dahlsten³, Yanni Sun², Po-Heng Lee⁴✉ & Giin Yu Amy Tan¹✉

Polyhydroxyalkanoates (PHAs) could be used to make sustainable, biodegradable plastics. However, the precise and accurate mechanistic modeling of PHA biosynthesis, especially medium-chain-length PHA (mcl-PHA), for yield improvement remains a challenge to biology. PHA biosynthesis is typically triggered by nitrogen limitation and tends to peak at an optimal carbon-to-nitrogen (C/N) ratio. Specifically, simulation of the underlying dynamic regulation mechanisms for PHA bioprocess is a bottleneck owing to surfeit model complexity and current modeling philosophies for uncertainty. To address this issue, we proposed a quantum-like decision-making model to encode gene expression and regulation events as hidden layers by the general transformation of a density matrix, which uses the interference of probability amplitudes to provide an empirical-level description for PHA biosynthesis. We implemented our framework modeling the biosynthesis of mcl-PHA in *Pseudomonas putida* with respect to external C/N ratios, showing its optimization production at maximum PHA production of 13.81% cell dry mass (CDM) at the C/N ratio of 40:1. The results also suggest the degree of *P. putida*'s preference in channeling carbon towards PHA production as part of the bacterium's adaptive behavior to nutrient stress using quantum formalism. Generic parameters (k_D , k_N and θ) obtained based on such quantum formulation, representing *P. putida*'s PHA biosynthesis with respect to external C/N ratios, was discussed. This work offers a new perspective on the use of quantum theory for PHA production, demonstrating its application potential for other bioprocesses.

Polyhydroxyalkanoates (PHAs) are naturally occurring biopolymers synthesized by some microorganisms as an intracellular energy reservoir in the face of nutrient stress, typically under imbalanced nutrient conditions such as high carbon-to-nitrogen (C/N) and high carbon-to-phosphorus (C/P) ratios^{1,2}. As PHAs possess favorable chemical properties³, are chemically stable and also easily biodegradable at the end of their lifecycle³, they have the potential to replace traditional plastics. Yet, despite their promising applications, the commercialization of PHAs, particularly medium-chain-length PHA (mcl-PHA), is hindered by high production costs due to the complexity of optimizing biosynthesis for industrial bacterial populations^{4,5}.

Under the microscope, it is observed that isogenic bacterial populations would differentiate into subpopulations to occupy different metabolic states and display varying phenotypes due to stochastic dynamics in the environment, intrinsic genetic factors, and survival strategies^{6,7}. This phenomenon has also been observed in PHA-producing bacteria by us and others where heterogeneity in PHA production is found in pure bacterial cultures⁸. Understanding how such heterogeneity occurs could lead to new PHA optimization strategies.

Decision-making in bacteria, or in any cellular organism, occurs when they exhibit different fates even when subjected to the same genetic or environmental condition^{9–11}, we can therefore view PHA production in *P. putida* as a decision-making process, where each bacterium makes a decision of producing PHA based on its external environment and internal genetic parameters. One can model such decision-making process as a stochastic model with Markov property, where each immediate future state is dependent on its immediate prior

¹Department of Architecture and Civil Engineering, City University of Hong Kong, Hong Kong SAR, China. ²Department of Electrical Engineering, City University of Hong Kong, Hong Kong SAR, China. ³Department of Physics, City University of Hong Kong, Hong Kong SAR, China. ⁴Department of Civil and Environmental Engineering, Imperial College London, London, UK. ✉email: po-heng.lee@imperial.ac.uk; amytan@cityu.edu.hk

state¹², and change is then modelled as a series of transitions between states, where probabilities are assigned to define such transitions.

This classical interpretation of decision-making contains the philosophy of *mechanism*, which is in turn rooted under molecular biology¹³: a cellular organism is seen as a complex, well-planned machine modelled by evolution, its structure and underlying rule set capable of being comprehended with reductionistic terms. Each transformation in the decision-making process reflects a specific series of responses within the biochemical mechanisms of the bacterial cell.

However, states of uncertainty arise from the complexity of biochemical processes in bacteria: the production and degradation of PHA are interconnected with the central carbon metabolism, resulting in a dynamic cycle that influences various bacterial processes, including stress response, pathogenesis, and persistence². PHA metabolism in microorganisms is influenced by multiple regulatory networks, including global and specific regulators which are also connected to various carbon cycles¹¹. These regulatory mechanisms are inherently complex, composing multiple regulatory networks intertwined across different scales in time and space^{14–17}. This complexity, owing to its metabolism regulation mechanism, give rise to uncertain states that are hard to capture under the classical mechanistic interpretation of decision-making. One example would be when nitrogen stress is insufficient to stimulate the production of PHA, but the necessary biochemical constituents are being synthesized and ready for PHA production; such would be a scenario of *neither quiescent nor producing*, an in-between, uncertain state that is hard to be explicitly modelled for classical decision-making models, requiring more information about its internal workings beforehand.

Considering these challenges, an alternative to describe uncertain decision-making within bacterial cells is needed. Quantum theory has been regarded as a highly successful theory of the twentieth century in modeling probabilistic behavior. It has been used for describing macro-level classical processes in biological systems^{18–20}. For example, Asano, et al.¹⁸ formulated a quantum-like decision-making model that simulated the genetic regulation underlying *E. coli*'s adaptive diauxic behavior towards lactose and glucose utilization. The authors considered bacteria as decision makers that are quantum-like, meaning that uncertainty (e.g. glucose and/or lactose uptake) can be modelled by superposition of event states.

Based on the approach by Asano, et al.¹⁸, we developed a quantum-like decision-making model capable for modeling bacterial PHA biosynthesis. The model is formulated by the “preparation” of nutrient condition detection and activation of gene regulation as the inputs (i.e., C/N ratios and a “hidden” genetic preference parameter), followed by “transformation” and “measurement” of physiological outputs responding to previous inputs (i.e., PHA production). This formulation of “preparation”, “transformation” and “measurement” embeds gene expression and regulation events into a 2-stage quantum-like decision-making model. The system to be modelled can therefore be described as the transformation of a density matrix. To validate the model, we performed experiments on the bacterium *P. putida* by feeding a range of C/N ratios, representing a spectrum of nutrient conditions to simulate low to high nutrient stress environments, and quantified PHA accumulation response associated with each C/N ratio. Parameters (k_D , k_N and theta θ) obtained from the modeling results of PHA biosynthesis based on such quantum formulation were discussed. This work provides an accurate empirical-level description of the environmental nutrient effect on PHA production in *P. putida*.

Methods

PHA production and quantification

P. putida NBUS12, which was previously isolated and characterized by our group, is a bacterium capable of bioconverting monoaromatic substrate styrene to mcl-PHA under nitrogen-stress condition^{1,8} and was chosen as a model bacterium for this study. To induce PHA production, *P. putida* NBUS12 was cultivated in a 250 mL conical flask containing 50 mL of 1X mineral salt medium (MSM) at a final optical density at 600 nm (OD₆₀₀) of 0.1. Styrene and NH₄Cl were added as the sole carbon and nitrogen source, respectively. Nitrogen source was supplied in the form of NH₄Cl at 0.192 g/L (50 mg/L nitrogen) while styrene was supplied at varying amounts to a central glass column fused to the central base of the growth flasks to obtain C/N (g/g) ratios of 10:1, 20:1, 30:1, 40:1 and 50:1. The conical flasks were tightly-sealed and incubated at 30 °C with shaking at 180 rpm. After 48 h, the bacterial cultures were centrifuged (9840 g, 15 °C, 10 min) to harvest the cell pellets. Cell pellets were washed twice with 1X phosphate buffer saline (PBS) buffer and freeze-dried. The cell dry mass (CDM) of freeze-dried biomass was determined by weighing. PHA content was quantified by subjecting dried biomass (5–10 mg) to methanolysis, followed by GC–MS analysis according to the procedures described by Tan et al.¹. The experiment was conducted in triplicates.

Model conceptualization

From the experimental data collected, the input and output parameters for modeling were C/N ratio and average cellular PHA content, respectively. The nutrient condition processing by bacterial cells is a stochastic process where *P. putida* metabolizes carbon and nitrogen substrates, which meet the bacterial cell wall randomly as dictated by molecular kinetics. A nominal model that can be constructed is a cell with singular input (C/N ratio) and output (PHA content).

As illustrated in Fig. 1, there are four possible states—the bacterial cell (1) may or (2) may not detect limiting amounts of nitrogen in its immediate surroundings and (3) may or (4) may not produce PHA. The events of detection are denoted as “D” and “N”, representing the detection of nutrient stress condition and non-detection of nutrient stress (i.e., nitrogen-rich) condition, respectively. The events of gene activation are denoted as “+” and “–”, representing activation or non-activation of the PHA biosynthesis pathway to produce PHA, respectively.

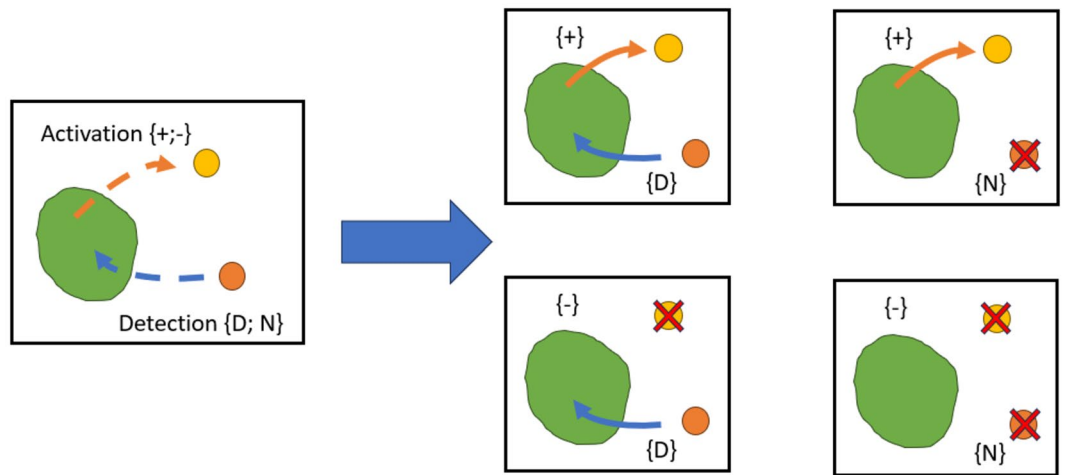


Figure 1. Four different cell states for PHA biosynthesis. The green object represents the bacteria, the yellow object represents PHA and the orange object represents nutrient stress condition. “D” and “N” denote the bacterium’s detection of nutrient-stress condition and non-detection of nutrient stress condition (i.e., nutrient-rich), respectively. “+” and “-” denote the activation or non-activation of the PHA biosynthetic pathway, respectively.

Quantum-like decision-making model

Based on the work of Asano et al.¹⁸, we assumed that a bacterial cell is a system which processes external environmental information in a “quantum-like” manner. By “quantum-like”, we imply that we do not couple actual quantum effects observed in sub-atomic scale events to biological processes, but rather, draw parallels between quantum probability, its philosophy and biological complexities to utilize advanced quantum theories for biology problems. We assume no more than the same conceptualization as depicted previously in Fig. 1, with a detection and activation stage. Any information processing is encoded in the transformation through the environmental nutrient condition detection operator (D) and gene activation operator (Q), which represents *P. putida* NBUS12’s adaptation to its environment (C/N ratio) and the state-change of PHA biosynthesis pathway brought on by gene regulation, respectively, which is illustrated by Fig. 2.

The quantum representation of nitrogen-induced PHA production by *P. putida* NBUS12 is described as a 2-stage quantum-like system by the general transformation of a density matrix ρ , given by Eq. (1):

$$\rho_{out} = \frac{V \rho_{in} V^*}{\text{tr}(V \rho_{in} V^*)} \quad (1)$$

where ρ_{in} represents the initial state of *P. putida* NBUS12 before nutrient condition detection where the bacteria have not received any external nutrient condition signal nor activated the expression of genes related to PHA biosynthesis. By encoding experimental measures and unobservable (i.e., hidden) genetic variables as quantum operators D and Q acting on the density matrix, we can derive the matrices ρ_D and ρ_Q which represent the transformed cell states of *P. putida* NBUS12 following the detection of C/N ratio and the subsequent gene regulation of PHA biosynthesis pathway, respectively. This enables us to simulate all the possible state outcomes depicted in Fig. 1. Such formalism also obeys the laws of quantum system dynamics, where the transformation follows the Lindblad equation for quantum dynamics¹⁸.

To simulate the potential biological states, we regard the bacteria as a decision maker which recognizes nutrient conditions as a superposition of events, given by Eq. (2):

$$|\psi_{in}\rangle = \alpha|e_1\rangle + \beta|e_2\rangle \quad \alpha, \beta \in \mathbb{C} \quad (2)$$

where the values of α^2 and β^2 correspond to the probabilities of arbitrary events e_1 and e_2 , respectively, which we will define as the detection of nutrient stress and nutrient-rich conditions, respectively, in subsequent sections.

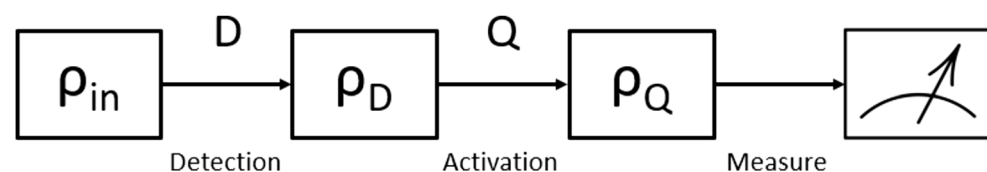


Figure 2. Schematics of a generic two-stage quantum-like model for decision-making modelling.

This notion of having both events considered in tandem utilizes the concept of quantum superposition, where the state of a bacteria is defined by both events, rather than just one event or the other¹⁸.

Initial stage

We introduce a state vector $|x_0\rangle$, given by Eq. (3):

$$|x_0\rangle = \frac{1}{\sqrt{2}}|e_1\rangle + \frac{1}{\sqrt{2}}|e_2\rangle = \frac{1}{\sqrt{2}}\begin{pmatrix} 1 \\ 1 \end{pmatrix} \quad (3)$$

The density matrix ρ_0 simulates the bacteria's initial cell state, given by Eq. (4):

$$\begin{aligned} \rho_0 &= |x_0\rangle\langle x_0| \\ \rho_0 &= \frac{1}{2}\begin{pmatrix} 1 & 1 \\ 1 & 1 \end{pmatrix} \end{aligned} \quad (4)$$

The bases $|e_1\rangle, |e_2\rangle$ correspond to the events of detection of nutrient stress condition P(D) and non-detection of nutrient stress condition P(N) (i.e., nutrient-rich), and $\frac{1}{\sqrt{2}}$ is the probability amplitude for the events, which when squared, becomes 0.5. This implies that the bacterial cell's recognition for nutrient condition is neutral at the beginning.

Nutrient condition detection stage

Given the operator D, which is a diagonal matrix containing the information of nutrient condition, the system state will transit from the initialization stage to the nutrient condition detection stage. Intuitively, the nutrient condition detection stage indicates that the cell has already detected if the environment is nutrient stress but has yet to activate its genes for PHA biosynthesis, given by Eq. (5):

$$D = \begin{pmatrix} \alpha & 0 \\ 0 & \beta \end{pmatrix} \quad (5)$$

Using Eq. (4) with operator D, the transformed density matrix is given by Eq. (6):

$$\rho_D = \begin{pmatrix} |\alpha|^2 & \alpha\beta^* \\ \alpha^*\beta & |\beta|^2 \end{pmatrix} \quad (6)$$

where α^2 represents the probability of the cell detecting nutrient stress, that is P(D), and β^2 indicates the probability of detecting nutrient-rich, P(N), i.e., $\alpha^2 + \beta^2 = 1$.

Gene activation stage

After the nutrient condition detection stage, the cell would enter the gene activation stage. The operator Q indicates the gene expression mechanism in response to different nutrient conditions and is given by Eq. (7):

$$Q = \begin{pmatrix} a & b \\ c & d \end{pmatrix} \quad a, b, c, d \in \mathbb{C} \quad (7)$$

Using Eq. (1) with operator Q, the cell's state will transit to the gene activation stage, given by Eq. (8):

$$\rho_Q = \frac{1}{\sigma} \begin{pmatrix} |\alpha\alpha + b\beta|^2 & (\alpha\alpha + b\beta)(c\alpha + d\beta)^* \\ (\alpha\alpha + b\beta)^*(c\alpha + d\beta) & |c\alpha + d\beta|^2 \end{pmatrix} \quad (8)$$

where:

$$\sigma = |\alpha\alpha + b\beta|^2 + |c\alpha + d\beta|^2$$

Measurement of probabilities

The input and output information are represented as a compound system using lifting maps^{18,21}, where the representation by lifting gives a different method to calculate the joint probability of events. The premise of doing so is by considering that input and output information influence each other and should be considered as such in the mathematical formulation of probabilities. The lifting map for the cell system and the joint probabilities for the four possible detection and activation outcomes depicted are given by Eq. (9):

$$\begin{aligned} \varepsilon(\rho) &= \rho_q \otimes \rho_0 \\ P(+, D) &= \text{tr}(E_1 \otimes E_1)\varepsilon(\rho) \\ P(-, D) &= \text{tr}(E_2 \otimes E_1)\varepsilon(\rho) \\ P(+, N) &= \text{tr}(E_1 \otimes E_2)\varepsilon(\rho) \\ P(-, N) &= \text{tr}(E_2 \otimes E_2)\varepsilon(\rho) \end{aligned} \quad (9)$$

where E_1 and E_2 are projection operators, which when acted upon the lifting map, would enable us to obtain the joint probabilities corresponding to the various phenotypic outcomes:

$$E_1 = |e_1\rangle\langle e_1| = \begin{pmatrix} 1 & 0 \\ 0 & 0 \end{pmatrix}$$

$$E_2 = |e_2\rangle\langle e_2| = \begin{pmatrix} 0 & 0 \\ 0 & 1 \end{pmatrix}$$

Thus, the predicted production of PHA, $P(+)$, can be represented as the sum of probabilities $P(+, D)$ and $P(+, N)$, given by Eq. (10):

$$P(+) = \frac{|\alpha\alpha + b\beta|^2}{|\alpha\alpha + b\beta|^2 + |c\alpha + d\beta|^2} \quad (10)$$

Classical decision-making model

Using the same conceptualization and reasoning from the quantum formalism, we can describe the decision-making process of a bacterial cell in the classical fashion using a Markov chain as follows:

$$O = D \cdot Q \cdot S \quad (11)$$

where the final observation state matrix is denoted as O , the transient states of detection and gene activation are denoted as D and Q respectively, and the initial state of the bacterial cell is denoted as S .

The detection state matrix D and gene activation state matrix Q have the following forms:

$$D = \begin{pmatrix} \alpha & 0 \\ 0 & \beta \end{pmatrix}, Q = \begin{pmatrix} x & y \\ z & w \end{pmatrix}, \alpha, \beta, x, y, z, w \in \mathbb{R}^+ \quad (12)$$

The initial state matrix S_c has the form as follows:

$$S_c = \frac{1}{2} \begin{pmatrix} 1 \\ 1 \end{pmatrix} \quad (13)$$

where it represents the hidden state of bacteria, having no initial preference towards nutrient condition. This corresponds to the initial condition of an isogenic population before exposure to varying C/N ratios. The main difference between classical and quantum formalism lies in the preparation of the initial state: the quantum formalism prepares a density matrix to represent superposition of states, whereas classical formalism prepares a state vector to represent two discrete states.

The observation state matrix O for the classical model is as follows:

$$O_c = \frac{1}{2} \begin{pmatrix} x\alpha + z\beta \\ y\alpha + w\beta \end{pmatrix} \quad (14)$$

The first element of O would be the probability of $P(+)$ in the classical formalism:

$$P(+) = \frac{1}{2}(x\alpha + z\beta) \quad (15)$$

We would assume that the probability of $P(+)$ should be influenced by whether it detects nutrient stress or not, i.e., influenced by $P(D)$ and $P(N)$, and these probabilities should have correlation with nutrient condition, i.e. the higher the C/N ratio, the more probable the bacterial cell detection, vice versa. We can therefore rewrite Eq. (15) as follows:

$$\begin{aligned} \alpha &= \gamma \cdot P(D), \beta = \tau \cdot P(N) \\ P(+) &= \frac{1}{2}(x\gamma \cdot P(D) + z\tau \cdot P(N)) \end{aligned} \quad (16)$$

Results and discussion

P. putida NBUS12's PHA accumulation response to different C/N ratios

The PHA accumulation of *P. putida* NBUS12 was evaluated for different C/N ratios (Table 1). At low C/N ratio of 10:1, corresponding to a nutrient-rich condition, there was negligible level of PHA production (0.06 %CDM). However, at higher C/N ratios, simulating nutrient stress, intracellular PHA levels rose and peaked at 13.8 %CDM at a C/N ratio of 40:1. A further increase in C/N ratio to 50:1 resulted in a significant reduction in PHA accumulation (2.51 %CDM). Such a narrow window of C/N ratio with high PHA accumulation is well-known and has been widely reported. For example, in another styrene-degrading and PHA-producing bacterium *P. putida* CA-3 (NCIMB 41162), little to no PHA production was observed until the C/N ratio exceeded 14:1 with peak PHA production occurring at the C/N ratio 28:1²². Similar observations were also made for other aromatic and non-aromatic substrates in pure and mixed cultures^{23,24}. This complex PHA production response across species suggests randomness underlying macro-scale biological dynamics²⁰. This meant that rather than modeling *P. putida* NBUS12's PHA biosynthesis as a classical stochastic system with discrete input state spaces, it can be

C/N ratio	Average PHA content (%CDM)	s.d.
10: 1	0.06	0.03
20: 1	0.31	0.00
30: 1	4.53	0.35
40: 1	13.81	4.02
50: 1	2.51	1.71

Table 1. The relationship between C/N ratio and PHA production for *P. putida* NBUS12.

modeled as a quantum-like system in which both nutrient stress and nutrient-rich conditions affect the outcome of PHA formation.

Quantum-like model fitting with experimental data

The operators D and Q separately encode nutrient condition and internal gene regulation mechanisms, respectively, and we set the operators as identical mapping of the system input where P(D) signifies the event of nutrient stress detection and P(N) corresponds to the event of nutrient-rich detection; + and – corresponds to the event of PHA production and non-production, respectively.

Using the experimental data, we formulated Q by the generic parameters of k_D , k_N and theta θ , which are real numbers as follows:

$$Q = \begin{pmatrix} \sqrt{P(+|D)}k_D & \sqrt{P(+|N)}k_N e^{i\theta} \\ \sqrt{P(-|D)}k_D & \sqrt{P(-|N)}k_N e^{i\theta} \end{pmatrix} \quad (17)$$

$$Q = \begin{pmatrix} \sqrt{P(+|D)} & \sqrt{P(+|N)} \\ \sqrt{P(-|D)} & \sqrt{P(-|N)} \end{pmatrix} \begin{pmatrix} \sqrt{k_D} & 0 \\ 0 & \sqrt{k_N} e^{i\theta} \end{pmatrix} \quad (18)$$

As per the formulation by Asano et al.²¹, we reformulated P (+) as follows:

$$P(+)=\frac{P(+|D)P(D)\sqrt{\frac{k_D}{k_N}}+P(+|N)P(N)\sqrt{\frac{k_N}{k_D}}+2\tilde{\delta}\cos\theta}{P(D)\sqrt{\frac{k_D}{k_N}}+P(N)\sqrt{\frac{k_N}{k_D}}+2\tilde{\delta}\cos\theta} \quad (19)$$

where:

$$\tilde{\delta}=\sqrt{P(+|D)P(+|N)P(D)P(N)}$$

$$\tilde{\delta}=\sqrt{P(D)P(N)}\left[\sqrt{P(+|D)P(+|N)}+\sqrt{P(-|D)P(-|N)}\right]$$

As seen in Eqs. (16) and (19), the classical decision-making formalism considers events separately, whereas through the quantum formalism, there is a *combined consideration* of events in terms of multiplication of probability amplitudes.

The quantum-like and classical probabilities from the experimental data are calculated and provided in Supplementary Material. Based on the calculations, we plotted the calculated probability P (+) against each C/N ratio, given as Fig. 3.

Further, we found that the value of $\frac{k_D}{k_N}=0.29512$ and theta $\theta=\pi$ achieved a highly fitted model, with the residual sum of squares (SSE) being 0.0038, indicating high agreement with the experimental data.

Compared to the classical approach, our model uses probability amplitudes as per Born's rule²⁵, the application of quantum-like decision theory to cell activity is based on the recognition that cells exhibit certain quantum-like characteristics, such as the existence of uncertain, in-between states that can be modeled using a quantum framework, analogous to quantum superposition of states. This is shown through the different formulation of the initial states (i.e. two-state vector versus density matrix) between the classical and the quantum-like model. Through the quantum formalism representing gene expression and regulation events as hidden variables, we consider the detection of nutrient condition and subsequent metabolic rewiring to both exert influence towards the bacterium's cellular state. The matrix containing the parameters k_D , k_N and theta θ in Eq. (13) describes *P. putida* NBUS12's adaptation to external C/N ratios. This can be considered as an invariant quantity describing the bacteria's character in its adaptive metabolic rewiring for either PHA production or non-production. This is selective metabolism at play. The k_D to k_N ratio indicates the bacteria's preference of nutrient conditions for PHA production. More specifically, it modulates the bacteria's preference of C/N ratio for maximum PHA production. This interpretation is in line with the findings from multi-omics analysis of *P. putida* strains. Varying the C/N ratio has been reported to affect a significant number of gene and protein expressions implicated in PHA biosynthesis-related pathways including, amino acid metabolism, nitrogen scavenging, general cellular processes, and transcriptional regulation^{1,26}. For instance, under a lower C/N ratio, Crc protein suppresses PHA formation by inhibiting the translation of PHA polymerase, while at a higher C/N ratio this suppression is removed, facilitating PHA production²⁷. Nevertheless, such regulations are observed to be probabilistic as low amounts

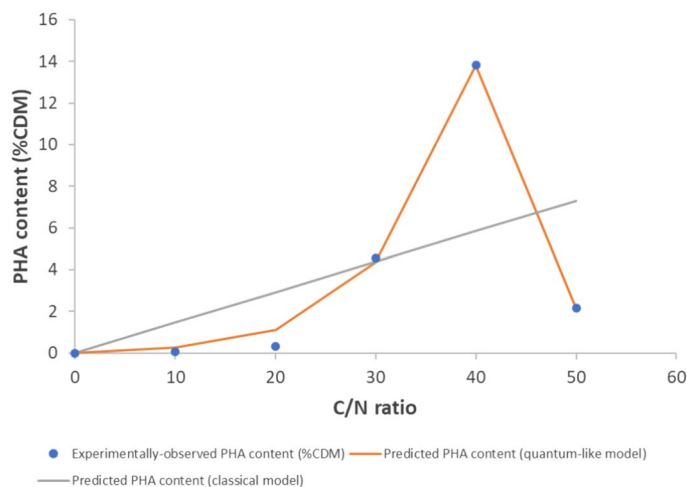


Figure 3. Predicted vs experimental PHA content at different C/N ratios.

of PHA are often detected at non-optimal C/N ratios. Hence, based on the interpretation of quantum theory, it is plausible that such destructive interference could be analogous to the interference between the probability amplitude of events, representing the cell's transitory genetic and metabolic states^{28,29}.

It was also observed that k_D to k_N ratio value could reflect non-PHA producers and PHA-producers that are unaffected by nutrient conditions. For example, very small to zero k_D to k_N ratio values would result in negligible to no production at all nutrient conditions, signifying that the bacterium is impartial to all nutrient conditions and does not activate PHA production. This reflects the scenario of a non-PHA producing bacteria. Conversely, very large values of k_D to k_N ratio (i.e., over 60) would lead to a low and basal level of PHA production at all nutrient conditions. This means that the bacterium has no preference of nutrient condition for PHA production, representing PHA-producing bacteria that accumulates the biopolymer alongside growth. Examples of such bacteria include some species of *Cupriavidus necator*, *Protomonas extorquens* and *Pseudomonas oleovorans*³⁰.

Overall, the conclusion obtained in this study is also supported by Asano, et al.'s work¹⁸, where different strains will have different preferences, i.e. different value ratios, towards glucose and lactose metabolism. However, due to the linearity of the quantum formalism, the understanding of k_D/k_N ratio for non-linear responses exhibited by complex biological systems would require further investigation. One possible method is the Generalized Probability Theory (GPT), one of the quantum information frameworks that cover both classical and quantum aspect³¹.

While such quantum formalism was first conceived to model the specific activation of a single gene operon in *E. coli*'s response to two different carbon substrates uptake¹⁸, we have successfully adapted and demonstrated the applicability of such formalism to model the whole cell's probabilistic adaptive behavior (i.e., PHA production) responding to environmental conditions (i.e., varying C/N ratios). This does not require a detailed model construction but rather, incorporates genomic regulation flow, i.e., cellular sensing, detection and gene regulation processes as the model's hidden variables. It, therefore, offers a novel perspective on the use of quantum formalism to investigate decision making and bioprocess modeling for PHA production and potentially, for other bioprocesses exhibiting similar non-linear, stochastic decision making in a quantum-like fashion. Moreover, employing quantum information theory to describe transcriptomics and proteomics data, which take account of genetic and regulation factors, could underpin event superposition and uncertainty of the system, ultimately revealing new insights on gene regulation in the future. Formulating systems with complex data such as multi-omics and physiological performance in a quantum-like manner means that such systems could be implemented onto quantum computers. This would benefit the development of multiple information layer modeling for systems with pure and mixed cultures in the future.

Conclusion

Microbial-based PHAs are excellent carbon-neutral substitutes for petroleum-based plastics and are also commercially valued for their potential biomedical and pharmaceutical applications. However, PHA production has yet to be maximized. This hinders its commercialization potential, particularly for mcl-PHA. Instead of modeling PHA formation based on classical decision-making approaches, we developed a model for mcl-PHA biosynthesis by the quantum formalism, introducing the "preparation" of nutrient condition detection and activation of gene regulation in response to environment inputs (i.e., C/N ratio) followed by "transformation" and "measurement" of PHA production. A 2-stage quantum-like decision-making model was formulated and the simulation results were in agreement with the experimental results for C//N ratios between 10:1 and 50:1. We also determined a new invariant quantity (given by $\theta = \pi$ and k_D/k_N ratio). These parameters described the interference between the probability amplitude of events during adaptive dynamics and allow us to quantitatively estimate *P. putida* NBUS12's PHA production adaptation to extracellular C/N ratios. This work offers an empirical-level description for PHA formation and may be further adapted to other bioprocesses for physiological optimization, especially for non-discrete (quantum-like) metabolic phenomena.

Data availability

All data generated or analysed during this study are included in this published article and its Supplementary Materials.

Received: 7 December 2023; Accepted: 26 July 2024

Published online: 06 August 2024

References

1. Tan, G.-Y.A. *et al.* Start a research on biopolymer polyhydroxyalkanoate (PHA): A review. *Polymers* **6**, 706–754 (2014).
2. Manoli, M.-T., Nogales, J. & Prieto, A. Synthetic control of metabolic states in *Pseudomonas putida* by tuning polyhydroxyalkanoate cycle. *Mbio* **13**, e01794-e11721 (2022).
3. Nanda, S., Patra, B. R., Patel, R., Bakos, J. & Dalai, A. K. Innovations in applications and prospects of bioplastics and biopolymers: A review. *Environ. Chem. Lett.* **20**, 379–395 (2022).
4. Lee, J., Park, H. J., Moon, M., Lee, J.-S. & Min, K. Recent progress and challenges in microbial polyhydroxybutyrate (PHB) production from CO₂ as a sustainable feedstock: A state-of-the-art review. *Bioresour. Technol.* **339**, 125616 (2021).
5. Chen, G.-Q., Chen, X.-Y., Wu, F.-Q. & Chen, J.-C. Polyhydroxyalkanoates (PHA) toward cost competitiveness and functionality. *Adv. Ind. Eng. Polym. Res.* **3**, 1–7 (2020).
6. Solopova, A. *et al.* Bet-hedging during bacterial diauxic shift. *Proc. Natl. Acad. Sci.* **111**, 7427–7432 (2014).
7. Kotte, O., Volkmer, B., Radzikowski, J. L. & Heinemann, M. Phenotypic bistability in *Escherichia coli*'s central carbon metabolism. *Mol. Syst. Biol.* **10**, 736 (2014).
8. Tan, G.-Y.A. *et al.* Bioconversion of styrene to poly (hydroxyalkanoate)(PHA) by the new bacterial strain *Pseudomonas putida* NBUS12. *Microbes Environ.* **30**, 76–85 (2015).
9. Thattai, M. & Van Oudenaarden, A. Intrinsic noise in gene regulatory networks. *Proc. Natl. Acad. Sci.* **98**, 8614–8619 (2001).
10. Raj, A. & Van Oudenaarden, A. Nature, nurture, or chance: Stochastic gene expression and its consequences. *Cell* **135**, 216–226 (2008).
11. Balázsi, G., Van Oudenaarden, A. & Collins, J. J. Cellular decision making and biological noise: From microbes to mammals. *Cell* **144**, 910–925 (2011).
12. Yoon, B.-J. Hidden Markov models and their applications in biological sequence analysis. *Curr. Genom.* **10**, 402–415 (2009).
13. Nicholson, D. J. Is the cell really a machine?. *J. Theor. Biol.* **477**, 108–126 (2019).
14. Stubbe, J. *et al.* Nontemplate-dependent polymerization processes: Polyhydroxyalkanoate synthases as a paradigm. *Annu. Rev. Biochem.* **74**, 433–480 (2005).
15. Pardelha, F., Albuquerque, M. G., Reis, M. A., Oliveira, R. & Dias, J. M. Dynamic metabolic modelling of volatile fatty acids conversion to polyhydroxyalkanoates by a mixed microbial culture. *New Biotechnol.* **31**, 335–344 (2014).
16. Peregrina, A., Martins-Lourenço, J., Freitas, F., Reis, M. A. & Arraiano, C. M. Post-transcriptional control in the regulation of polyhydroxyalkanoates synthesis. *Life* **11**, 853 (2021).
17. Mitra, R., Xu, T., Chen, G. Q., Xiang, H. & Han, J. An updated overview on the regulatory circuits of polyhydroxyalkanoates synthesis. *Microb. Biotechnol.* **15**, 1446–1470 (2022).
18. Asano, M. *et al.* Quantum-like model of diauxie in *Escherichia coli*: Operational description of precultivation effect. *J. Theor. Biol.* **314**, 130–137 (2012).
19. Khrennikov, A. Quantum Bayesianism as the basis of general theory of decision-making. *Philos. Trans. R. Soc. A: Math. Phys. Eng.* **374**, 20150245 (2016).
20. Basieva, I., Khrennikov, A. & Ozawa, M. Quantum-like modeling in biology with open quantum systems and instruments. *Bio-systems* **201**, 104328 (2021).
21. Accardi, L. & Ohya, M. Compound channels, transition expectations, and liftings. *Appl. Math. Optimiz.* **39**, 33–59 (1999).
22. Ward, P. G., de Roo, G. & O'Connor, K. E. Accumulation of polyhydroxyalkanoate from styrene and phenylacetic acid by *Pseudomonas putida* CA-3. *Appl. Environ. Microbiol.* **71**, 2046–2052 (2005).
23. Tan, G.-Y.A. *et al.* Enhanced gas chromatography-mass spectrometry method for bacterial polyhydroxyalkanoates analysis. *J. Biosci. Bioeng.* **117**, 379–382 (2014).
24. Albuquerque, M., Martino, V., Pollet, E., Avérous, L. & Reis, M. Mixed culture polyhydroxyalkanoate (PHA) production from volatile fatty acid (VFA)-rich streams: Effect of substrate composition and feeding regime on PHA productivity, composition and properties. *J. Biotechnol.* **151**, 66–76 (2011).
25. Born, M. Quantum mechanics of collision processes. *Uspekhi Fizich* **1926**, 456 (1926).
26. Poli, A., Di Donato, P., Abbamondi, G. R. & Nicolaus, B. Synthesis, production, and biotechnological applications of exopolysaccharides and polyhydroxyalkanoates by archaea. *Archaea* **2011**, 1–13 (2011).
27. La Rosa, R., de la Peña, F., Prieto, M. A. & Rojo, F. The Crc protein inhibits the production of polyhydroxyalkanoates in *Pseudomonas putida* under balanced carbon/nitrogen growth conditions. *Environ. Microbiol.* **16**, 278–290 (2014).
28. Prieto, A. *et al.* A holistic view of polyhydroxyalkanoate metabolism in *Pseudomonas putida*. *Environ. Microbiol.* **18**, 341–357 (2016).
29. Yukalov, V. I. & Sornette, D. Quantum probability and quantum decision-making. *Philos. Trans. R. Soc. A: Math. Phys. Eng. Sci.* **374**, 20150100 (2016).
30. Lee, Y. S. Plastic bacteria? Progress and prospects for polyhydroxyalkanoate production in bacteria. *Trends Biotechnol.* **14**, 431–438 (1996).
31. Mana, P. G. Why can states and measurement outcomes be represented as vectors? *arXiv preprint quant-ph/0305117* (2003).

Acknowledgements

The authors wish to acknowledge the Hong Kong Research Grants Council (RGC) General Research Fund (17208121, 17205322 and 11304920), University Grants Committee Research Matching Grant Scheme (UGC RMGS) of Hong Kong, the National Natural Science Foundation of China (Grant No. 11874312), and City University of Hong Kong (Project No. 9610623) for providing financial support.

Author contributions

L.Y.L.H. and P.L. wrote the main manuscript. L.Y.L.H. prepared Figs. 1 and 2. L.Y.L.H. and K.T.M.H. prepared Fig. 3. L.Y.L.H., M.F., F.Y.L., H.I.L., and G.B. formulated and validated the equations. G.Y.A.T. and M.T.W. provided data in Table 1. All authors reviewed the manuscript.

Competing interests

The authors declare no competing interests.

Additional information

Supplementary Information The online version contains supplementary material available at <https://doi.org/10.1038/s41598-024-68727-7>.

Correspondence and requests for materials should be addressed to P.-H.L. or G.Y.A.T.

Reprints and permissions information is available at www.nature.com/reprints.

Publisher's note Springer Nature remains neutral with regard to jurisdictional claims in published maps and institutional affiliations.

Open Access This article is licensed under a Creative Commons Attribution-NonCommercial-NoDerivatives 4.0 International License, which permits any non-commercial use, sharing, distribution and reproduction in any medium or format, as long as you give appropriate credit to the original author(s) and the source, provide a link to the Creative Commons licence, and indicate if you modified the licensed material. You do not have permission under this licence to share adapted material derived from this article or parts of it. The images or other third party material in this article are included in the article's Creative Commons licence, unless indicated otherwise in a credit line to the material. If material is not included in the article's Creative Commons licence and your intended use is not permitted by statutory regulation or exceeds the permitted use, you will need to obtain permission directly from the copyright holder. To view a copy of this licence, visit <http://creativecommons.org/licenses/by-nc-nd/4.0/>.

© The Author(s) 2024